

# Nanoscale

Accepted Manuscript



This is an *Accepted Manuscript*, which has been through the Royal Society of Chemistry peer review process and has been accepted for publication.

*Accepted Manuscripts* are published online shortly after acceptance, before technical editing, formatting and proof reading. Using this free service, authors can make their results available to the community, in citable form, before we publish the edited article. We will replace this *Accepted Manuscript* with the edited and formatted *Advance Article* as soon as it is available.

You can find more information about *Accepted Manuscripts* in the [Information for Authors](#).

Please note that technical editing may introduce minor changes to the text and/or graphics, which may alter content. The journal's standard [Terms & Conditions](#) and the [Ethical guidelines](#) still apply. In no event shall the Royal Society of Chemistry be held responsible for any errors or omissions in this *Accepted Manuscript* or any consequences arising from the use of any information it contains.

**Chondroitin sulfate-polyethylenimine copolymer-coated  
superparamagnetic iron oxide nanoparticles as an efficient  
magneto-gene carrier for microRNA-encoding plasmid DNA  
delivery**

Yu-Lun Lo<sup>1</sup>, Han-Lin Chou<sup>2</sup>, Zi-Xian Liao<sup>3</sup>, Shih-Jer Huang<sup>1</sup>, Jyun-Han Ke<sup>1</sup>, Yu-Sheng Liu<sup>1,4</sup>,  
Chien-Chih Chiu<sup>2</sup> and Li-Fang Wang<sup>1,2,3\*</sup>

<sup>1</sup>*Department of Medicinal & Applied Chemistry, College of Life Science, Kaohsiung Medical  
University, Kaohsiung 80708, Taiwan*

<sup>2</sup>*Department of Biotechnology, College of Life Science, Kaohsiung Medical University,  
Kaohsiung 80708, Taiwan*

<sup>3</sup>*Institute of Medical Science and Technology, National Sun Yat-Sen University, Kaohsiung 804,  
Taiwan*

<sup>4</sup>*School of Pharmacy Kaohsiung Medical University, Kaohsiung 80708, Taiwan*

---

**\*Correspondence to: Li-Fang Wang, Professor of Medicinal & Applied Chemistry**

Kaohsiung Medical University

College of Life Science

100 Shih-Chuan 1st Road, Kaohsiung City 80708, Taiwan

**Tel:** 886-7-312-1101 ext. 2217

**Fax:** 886-7-312-5339

**E-mail:** lfwang@kmu.edu.tw

Manuscript submitted to *Nanoscale* on March 02, 2015.

revised on March 25, 2015.

## ABSTRACT

MicroRNA-128 (miR-128) is an attractively therapeutic molecule with powerful regulation in glioblastoma. However, miR-128 lacks biological stability and leads to poor delivery efficacy in clinical applications. In previous study, we demonstrated two effective transgene carriers, including polyethylenimine (PEI)-decorated superparamagnetic iron oxide nanoparticles (SPION) as well as chemically-conjugated chondroitin sulfate-PEI copolymers (CP). In this contribution, an optimized condition is found to coat CP onto the surface of SPION named CPIO for magneto-gene delivery systems. The optimized weight ratio of CP and SPION is 2:1, forming a stable particle as a good transgene carrier. The hydrodynamic diameter of CPIO is  $\sim 136$  nm. The gel electrophoresis result demonstrates the weight ratio of CPIO/DNA to completely encapsulate pDNA is  $\geq 3$ . The *in vitro* tests of CPIO/DNA are done in 293T, CRL5802, and U87-MG cells in the presence and absence of an external magnetic field. The magnetofection efficiency of CPIO/DNA is measured in the three cell lines with or without fetal bovine serum (FBS). CPIO/DNA exhibits remarkably improved gene expression in the presence of the magnetic field and 10% FBS as compared with a gold non-viral standard, PEI/DNA, and a commercial magnetofection reagent, PolyMag/DNA. In addition, CPIO/DNA shows less cytotoxicity than do PEI/DNA and PolyMag/DNA against the three cell lines. The transfection efficiency of the magnetoplex improves significantly with an assisted magnetic field. In miR-128 delivery, a microRNA plate array and fluorescence in situ hybridization are used to demonstrate CPIO/pMIRNA-128 indeed expresses higher miR-128 with the assisted magnetic field than without. In a biodistribution test, CPIO/Cy5-DNA shows higher accumulation at the tumor site where an external magnet is placed nearby.

**Keywords:** *Magnetofection, MicroRNA, Glioblastoma, Gene delivery*

## INTRODUCTION

Glioblastoma multiform (GBM) is a highly malignant and incurable cancer developing from the brain with dismal prognosis and an extremely low percentage of survivors. Currently, GBM is classified to be the lethal form of grade IV glioblastomas according to the World Health Organization (WHO).<sup>1</sup> Although GBM rarely metastasizes, its invasive nature causes extensive infiltration of surrounding brain tissues. Because of this unique and uncontrollable character of GBM, it is difficult to remove glioblastomas completely by surgery.<sup>2</sup> Consequently, an anticancer drug can be used to treat GBM but its therapeutic outcome is also limited because hydrophobic drugs have difficulty passing the Blood-Brain Barrier (BBB).<sup>3</sup> Pardridge et al. reported most of the large molecular drugs and over 98% of small drugs could not enter brain tissue due to low permeability.<sup>3-6</sup> Therefore, the development of gene therapy combining a traditionally standard cure in treating GBM is considered a promising strategy.<sup>1</sup>

Gene therapy shows great potential in the treatment of a wide range of cancers, especially in glioblastomas, because of its innovative strategies and high specificity.<sup>7</sup> The treatment of glioblastomas includes strategies to deliver tumor-suppressor genes, suicide genes, immune response-induced cytokine genes, and conditionally replicating oncolytic viruses.<sup>1</sup> However, successful gene therapy needs to construct a perfect delivery system to ensure therapeutic genes delivered to a disease site and to avoid naked genes being degraded. This achievement depends

on the role of an effective gene carrier to enhance the circulation time of therapeutic genes.

There are two kinds of gene carriers, including viral and non-viral vectors. Although viral vectors show excellent transfection efficiency, however, they cannot be largely applied in clinics because of limited DNA packing cargo size and safety issues.<sup>7-9</sup> In contrast to viral vectors, non-viral vectors such as cationic polymers have potential in transferring larger gene sequence capacity and are more easily synthesized. In addition, non-viral vectors have advantages of low immune response and no pathogenesis.<sup>9-11</sup> Nevertheless, non-viral vectors still have to overcome the disadvantage of poor transfection efficiency relative to viral vectors.

Several strategies including NIR-mediated photo-release, ultrasound-mediated sonoporation, and magnetofection are used to supply an external stimulus to help vectors increase gene expression. However, current photolysis delivery systems always use short wavelength irradiation, which induces unavoidable cellular damage. This handicap limits the application of photo-reactive mediated delivery.<sup>9,12</sup> Sonoporation also has the drawback of instability of vectors that lead to unfavorable gene transfer efficiency because of the short lifetime of sonoporation microbubbles.<sup>13,14</sup> In contrast, magnetofection is considered an ideal method for rapid and highly efficient transfection. Magnetic targeting guides therapeutic genes to the desired tissues and has been evaluated in the treatment of many cancers.<sup>15,16</sup>

Magnetofection based on superparamagnetic iron oxide nanoparticles (SPION) carrying

plasmid DNA or small interfering RNA can improve the accumulation of nucleic acids at a specific area with an external magnetic field, resulting in enhanced gene expression, even up to several hundred fold.<sup>17-20</sup> In our previous study, cationic magnetic particles such as polyethylenimine (PEI)-coated SPION<sup>21</sup> and poly(N,N-dimethylaminoethyl methacrylate) (PDMAEMA)-grafted from the surface of iron oxide nanoparticles,<sup>17</sup> were demonstrated to be efficient magnetoplexes for plasmid DNA delivery. Magnetofection efficiency of the magnetoplexes performed in HEK 293T cells or U87 cells with or without 10% FBS, showed significant enhancement with an external magnetic field. In addition, the cationic polymers-coated SPION reduced cytotoxicity as compared with the cationic polymers themselves. It seems the combination of a cationic polymer and SPION for magnetofection is an attractive strategy in treating GBM owing to its guidance ability and gene expression enhancement.

MicroRNAs (miRNAs) are small, non-coding, endogenous RNAs containing 18 - 24 nucleotides in length that have biological functions in regulating cell development, proliferation, differentiation, motility and apoptosis through miRNA to mRNA binding mediated gene silence.<sup>22,23</sup> Several miRNAs were used to investigate their capability to suppress tumor growth and the invasion of GBM.<sup>24-29</sup> In this contribution, we focused on miR-128, a brain-enriched miRNA, down-regulates in gliomas such as U87-MG.<sup>25</sup> Recently, researchers showed overexpression of miR-128 in glioma reduced cell proliferation.<sup>25, 26, 30, 31</sup> Nevertheless, a

single-strand miRNA lacks stability and often encounters rapid degradation in serum environment.<sup>32</sup> In our previous study, we synthesized a low-cytotoxic and highly efficient cationic polymer as a pDNA delivery carrier, named chondroitin sulfate-polyethylenimine (CS-PEI, CP) with a CD44 targeting ability.<sup>33</sup> The CS moiety in CP provides a CD44-targeting feature, similar to hyaluronic acid (HA)<sup>34, 35</sup> and reduces the cytotoxicity of PEI. The CD44 targeting moiety-CS also offers a possibility in crossing BBB. It has been reported not only gliomas express the CD44<sup>36-39</sup> but mainly the component of the BBB, brain microvascular endothelial cells (BMEC) do.<sup>40, 41</sup> As previously mentioned, invasion is the commonest behavior of GBM and this infiltrative invasion has been demonstrated to involve CD44 expression.<sup>42</sup> Thus, CP seems a promising miR-128 carrier because CD44 is a good targeting moiety for GBM therapy.

To construct a magnetofection gene carrier for GBM therapy, CP was used to coat onto the surface of SPION named CPIO as a magneto-guide gene delivery system for further enhancement of gene expression when an external magnetic field was applied. CPIO was prepared by complexation through electrostatic interactions between CP and poly(acrylic acid)-bound iron oxide nanoparticles (PAAIO). The different w/w ratios of CPIO/pDNA were prepared to test the DNA condensation ability using a gel electrophoresis assay. The *in vitro* cell tests of CPIO/DNA were done in 293T, CRL5802, and U87-MG cells in the presence and absence of an external

magnetic field. The internalization of CPIO/pDNA with or without the magnetic field was analyzed using flow cytometry and confocal laser scanning microscopy. For miRNA delivery, we constructed a pDNA containing miR-128 precursor sequence and transfected it into U87 cells. The miRNA expression was tested using a miRNA plate assay kit and fluorescence in situ hybridization (FISH). To demonstrate the enhanced accumulation of CPIO/DNA at the tumor site where an external magnet was placed nearby, we labeled pDNA with a Cy5 dye and traced its fluorescence intensity using an U87-xenograft nude mouse model.

## **MATERIALS AND METHOD**

### **Materials**

Sodium chondroitin sulfate (CS) was purchased from Tohoku Miyagi Pharmaceutical Co., Ltd. (Tokyo, Japan). Methacrylic anhydride was purchased from Lancaster (Lancashire, UK) and used as received. Polyethylenimine (PEI, Mw= 10K and 25K Dalton) were purchased from Sigma-Aldrich (St. Louis, MO). Iron(III) chloride, anhydrous ( $\text{FeCl}_3$ ), sodium hydroxide, and poly(acrylic acid) (PAA, Mw= 2000 g/mol) were from TCI (Tokyo, Japan). Ethidium bromide (EtBr) was purchased from MP Biomedicals (Verona, Italy). Fetal bovine serum (FBS) was from Biological Industries (Beit Haemek, Israel). 3-(4,5-Dimethyl-thiazol-2-yl)-2,5-diphenyl-tetrazolium bromide (MTT) was from MP Biomedicals (Eschwege, Germany). Phosphate buffer

saline (PBS), Dulbecco's modified Eagle medium (DMEM), Minimum essential medium (MEM), trypsin–EDTA and Lipofectamine 2000 were purchased from Invitrogen (Carlsbad, CA). PolyMag was acquired from Chemicell GmbH (Berlin, Germany). A luciferase assay kit and lysis buffer were from Promega (Madison, WI). A BCA protein assay kit was from Thermo Fisher Scientific Inc. (Rockford, IL). A label IT nucleic acid labeling kit was purchased from Mirus Bio. (Madison, WI). A lentivector-based miR-128 precursor construct was purchased from System Biosciences Inc. (Mountain View, CA). Plasmid DNA (pDNA) was propagated in a chemically competent *E. coli* strain DH5 $\alpha$  (Yeastern biotech, Taipei, Taiwan), and purified using a Geneaid plasmids maxi kit (New Taipei City, Taiwan). Purity of pDNA was certified by the absorbance ratio at OD260/OD280, and by distinctive bands of DNA fragments at corresponding base pairs in gel electrophoresis after restriction enzyme treatments. A miR-128 plate assay kit was purchased from Signosis (Santa Clara, CA). All other unstated chemicals were purchased from Sigma chemical company (St. Louis, MO) and used without any further purification.

### **Preparing PEI-conjugated chondroitin sulfate (CP)**

Methacrylated CS (CSMA) was synthesized as previously described.<sup>43</sup> The degree of methacrylation on CS was controlled at 70%. PEI was grafted onto the CSMA using a molar ratio of 1.2 : 1 via a Michael addition. After PEI was completely dissolved in double deionized (DD)

water, the aqueous solution of CSMA (1 mg/mL) was added dropwise to the PEI solution (1 mg/mL) and stirred at room temperature (RT) for 48 h. The resulting crude product was purified by precipitation using acetone as a non-solvent. The precipitate was dissolved in DD water and further purified by dialysis using a dialysis membrane (MWCO 25K; Spectrum Labs, Rancho Dominguez, CA) against DD water for 3 days. The final product was obtained by lyophilization.

### **Preparing PAAIO and CP-coated PAAIO (CPIO).**

PAAIO was synthesized according to our previous publications.<sup>44, 45</sup> CP-coated PAAIO was prepared by mixing CP and PAAIO at various weight ratios from their individual stock solution at 2 mg/mL in DD water. Briefly, different weight ratios of CP and PAAIO were mixed and ultrasonicated (frequency 43K Hz, model D80H; Delta, Taipei, Taiwan) for 30 min.<sup>21</sup> The unbound CP was removed by placing a permanent magnet (Nd-Fe-B of 6000 G; Taiwan Magnet Co., Taipei, Taiwan) near the vial and the supernatant solution was carefully withdrawn. The magnetic-attracted CPIO complex was redispersed in 10 mL DD water and the supernatant solution was removed repeatedly by placing a permanent magnet. This purification procedure was done three times and CPIO was dried in a vacuum oven. In later studies, any interested concentration was prepared by dispersing the dried CPIO in DD water of pH 6.8.

### Preparing and characterizing CPIO/pDNA magnetoplexes

pEGFP-C1, pGL3-control, and pMIRNA-128 plasmids were introduced into *E. coli* strain DH5 $\alpha$  and propagated. Plasmid DNA (pDNA) was extracted using a maxi kit. CPIO and pDNA were dissolved in DD water, respectively, to a final concentration of 1 mg/mL. Plasmid DNA concentration was fixed at 3  $\mu$ g/100  $\mu$ L in DD water to measure DNA binding and 4  $\mu$ g/500  $\mu$ L for other measurements. Equal volumes of CP and pDNA solutions with various weight ratios (w/w) were mixed and immediately vortexed at a high speed for 60 s. The DNA binding ability of magnetoplexes was evaluated using an agarose gel electrophoresis with 0.8% agarose in Tris-acetate-EDTA (TAE) containing ethidium bromide (EtBr) (1  $\mu$ g/mL). A current of 100 V was applied to gels for 40 min, and DNA retention was visualized under UV illumination at 365 nm. To measure the resistance of magnetoplexes to DNase I, 1 unit of the enzyme was mixed with magnetoplexes and incubated for 1 h. The enzyme was inactivated by adding 150mM EDTA and incubating at 65 $^{\circ}$ C for 30 min. After that, a 25% (w/v) heparin solution was used to release the DNA from magnetoplexes. The resistance capacity of CPIO/DNA was evaluated using the agarose gel electrophoresis.

The hydrodynamic diameters and zeta potentials of magnetoplexes were measured using a Zetasizer Nano ZS instrument (Malvern, Worcestershire, UK). Light scattering measurements were done with a laser at 633 nm and a 90 $^{\circ}$  scattering angle. Polystyrene nanospheres (220  $\pm$  6

nm and  $-50$  mV) were used to verify the performance of the instrument. The particle size and zeta potential of each magnetoplex was measured three times. The size and morphology of the magnetoplexes were observed using a transmission electron microscope (TEM, Jeol TEM-1200; Tokyo, Japan). A carbon-coated 200-mesh copper specimen grid was glow-discharged for 1.5 min. Ten microliters of magnetoplexes were deposited on a TEM grid and allowed to dry at RT for a week. Images were observed under an acceleration voltage of 60K eV and captured with a CCD camera.

### Cell experiments

U87 cells (a human glioblastoma cell line) were cultivated and maintained at  $37$  °C under humidified  $5\%$   $\text{CO}_2$  in MEM, supplemented with  $10\%$  fetal bovine serum (FBS),  $1\%$  sodium pyruvate and  $100$   $\mu\text{g}/\text{mL}$  penicillin-streptomycin. 293T (a human embryonic kidney cell line) and CRL-5802 cells (a human lung cancer cell line) were cultivated in DMEM, supplemented with  $10\%$  fetal bovine serum (FBS) and  $100$   $\mu\text{g}/\text{mL}$  penicillin-streptomycin. The medium was replenished every three days, and the cells were sub-cultured after they had reached  $95\%$  confluence.

293T, CRL-5802, and U87 cells were seeded in 96-well tissue culture plates at a density of  $5 \times 10^3$ /well in their corresponding medium containing  $10\%$  FBS. The cytotoxicity of CPIO ( $2.5$  -

100  $\mu\text{g/mL}$ ) was evaluated by determining cell viability after 24 h of incubation. The cytotoxicities of magnetoplexes were examined at various weight ratios of CPIO/pDNA for 48 h of post-incubation after they had been incubated at 37 °C for 20 min with (w) or without (w/o) the magnetic field. PEI-25K/DNA was prepared at an N/P ratio of 10 and PolyMag/DNA was prepared according to the manufacturer's protocol (4  $\mu\text{L}$  of PolyMag and 4  $\mu\text{g}$  of DNA) with an assisted magnetic field for 20 mins. The number of viable cells was determined by estimating their mitochondrial reductase activity using a tetrazolium-based colorimetric method.<sup>46</sup>

*In vitro* transgene expression was done in 293T, CRL-5802, and U87 cells at a density of  $1 \times 10^5$ /well in 12-well plates and incubated in MEM or DMEM medium containing 10% FBS for 24 h before transfection. The transfection efficiencies of magnetoplexes were measured and compared with naked DNA (a negative control) and PEI-25K/DNA and PolyMag/DNA (positive controls). Magnetoplexes with w/w ratios of 3 - 15 were prepared using various amounts of CPIO and a fixed pDNA amount of 4  $\mu\text{g}$  to a final volume of 500  $\mu\text{L}$ , which were added into MEM/DMEM-maintained cells. Following 20 min of incubation with or without placing a static magnetic array (Chemicell GmbH, Berlin, Germany) under the culture plate, the medium was replaced with 1 mL of fresh complete-medium and the cells were incubated for 48 h of post-transfection. Green fluorescence protein (GFP) expression was directly visualized using confocal laser scanning microscopy (CLSM, Fv 1000 CLSM; Olympus, Tokyo, Japan).

For a luciferase assay, the procedures stated above were repeated with or without using 10% FBS to determine the transfection efficiency in the three cell lines. To quantify the luciferase expression, the transfected cells were twice rinsed gently with 1 mL of 0.01 M PBS, added to a 200- $\mu$ L/well of  $1\times$  Gjolysis buffer (Promega, Madison, WI), and allowed to stand overnight at  $-20\text{ }^{\circ}\text{C}$ . Luciferase gene expression was measured using a microplate scintillation and luminescence counter (Zeiss Axiovert 200; Gottingen, Germany) after mixing the contents of a 50- $\mu$ L/well of lysate with the contents of a 50- $\mu$ L/well of luciferase assay substrate. The total protein content of the cell lysate was examined using a BCA protein assay kit according to the manufacturer's instructions. Luciferase activity was normalized with the total protein content (RLU/mg protein).

### **Cellular uptake**

The internalized iron amount of CPIO/pDNA magnetoplexes inside cells was quantified using an inductively coupled plasma-optical emission spectrometer (ICP-OES, Optima 7000DV; Perkin-Elmer, Boston, MA). The count of  $1 \times 10^5$  cells from each sample was analyzed for iron content. The protein content of the half cell lysate was examined using the BCA protein assay kit. The other half cell lysate was dissolved in HCl and incubated at  $70\text{ }^{\circ}\text{C}$  for 1 h. The final volume was adjusted to 3 mL for analysis. The iron content of samples were calculated based on an

Fe(NO<sub>3</sub>)<sub>3</sub> calibration curve. In addition, CPIO was conjugated with a fluorescent probe, FITC for tracing.<sup>33</sup> Briefly, 10 mg of CP in DD water were mixed with 1 mg of FITC isomer in DMSO and the mixture was stirred in the dark at RT for 24 h. Unconjugated FITC was removed by dialysis (MWCO 1 K) against DD water for two days. Subsequently, the dialyzed solution was filtered to remove undissolved byproducts followed by lyophilization. FITC-labeled CP was also used to coat onto PAAIO for cellular tracing studies.

U87 cells were seeded in 12-well culture plates at a density of  $1 \times 10^5$ /well in the medium containing 10% FBS and incubated for 24 h. The FITC-conjugated magnetoplex containing 4  $\mu$ g DNA was added to MEM-maintained U87 cells. Following 20 min of incubation, the cells were trypsinized, centrifuged, and resuspended in 1 mL of cold 0.01M PBS, and analyzed using a flow cytometer.

### **Confocal laser scanning microscope (CLSM)**

The cellular uptake of magnetoplexes was observed using a CLSM. U87 cells were seeded at a density of  $1.0 \times 10^5$ /well in 12-well plates containing one glass coverslip/well in MEM supplemented with 10% FBS, and incubated for 24 h. The magnetoplex was prepared at a w/w ratio of 5 using FITC-conjugated CPIO and the Cy5-labeled pGL3-control plasmid (Mirus Labelit Cy5 labeling kit; Fisher Scientific Company, Pittsburgh, PA). The cells were exposed to

the fluorescent magnetoplex at 37 °C for 20 min with or without a magnetic field. The medium containing the magnetoplex was removed and washed gently with 1 mL of 0.01M PBS at pH 7.4. The cell nuclei were stained with 5 µg/mL Hoechst 33342 (Invitrogen, Carlsbad, CA) for 30 min. Next, the cells were washed with 0.01M PBS and fixed with 3.7% paraformaldehyde for 15 min. The cells on a coverslip were washed 3 times with 0.01M PBS and mounted with a fluorescent mounting medium on a glass slide. Cell images were analyzed using Olympus CLSM software.

### **miRNA expression**

miRNA expression was determined by fluorescence *in situ* hybridization (FISH) and a miRNA plate assay kit (Signosis, Santa Clara, CA). For FISH, U87 cells were seeded at a density of  $3.0 \times 10^4$ /well in 24-well plates containing one glass coverslip/well in MEM supplemented with 10% FBS, and incubated for 24 h. The magnetoplex containing 2 µg pMIRNA-128 pDNA was added to MEM-maintained U87 cells with an assisted magnetic field for 20 min. Next, the medium was replaced with 1 mL of fresh complete-medium and the cells were incubated for 48 h post-transfection. The transfected U87 cells were washed with 0.01M PBS and fixed with 4% paraformaldehyde. Sequentially, coverslips containing the cells were washed with 2X SSC buffer (saline-sodium citrate buffer in DEPC water) three times and dehydrated through ethanol in 70%, 80%, 90%, and 100% sequentially. The antisense miR-128 sequence was labeled Cy5 dye with a

nucleic acid labeling kit as a probe and hybridized with the coverslip containing the cells at 37 °C overnight. After hybridization, the coverslip with the cells were stained with DAPI and mounted with a fluorescent mounting medium on a glass slide. Finally, the FISH slide was visualized using a TissueFAXs system (Tissuegnostics, Tarzana, CA). For miRNA plate assay, RNA was extracted from pMIRNA-128 transfected U87 cells with a TRIzol reagent (Invitrogen, Carlsbad, CA) according to the standard protocol. Collected RNA was analyzed with a Signosis' plate array (Signosis, Santa Clara, CA,) according to the manufacturer's protocol. Chemiluminescence was determined using a TopCount microplate scintillation and luminescence counter (PerkinElmer Life and Analytical Sciences, Boston, MA). The non-transfected cells were used as a control.

### **Western blot**

pMIRNA-128 transfected U87 cells were harvested and lysed by CytoBuster protein extraction buffer (Merck Millipore Life Science, Darmstadt, Germany). The protein content of the cell lysate was determined using a BCA protein assay kit. An equal amount of protein (40 µg) was separated using 10% SDS-PAGE gel and transferred to a nitrocellulose (NC) membrane. The NC membrane was blocked in blocking buffer (5% nonfat milk powder dissolved in Tris-buffered saline buffer containing 0.1% Tween20 [TBST]) at RT. Following 1 h of incubation, the blocked NC membrane was probed with a 1:1000 dilution of pAKT, AKT, and

Bax antibodies in 1% nonfat milk-TBST buffer at 4 °C overnight. The next day, the NC membrane was washed three times with TBST and incubated with 1:4000 dilution of a peroxidase-conjugated secondary antibody in TBST at RT for 1 h. The NC membrane was washed three times with TBST and developed using an enhanced chemiluminescence (ECL) detection system.

### **Biodistribution**

Nude mice (Balb/cAnN-Foxn1nu/CrlNarl, male, n=3) were subcutaneously injected with  $3 \times 10^6$  U87 cells in their right and left hind leg regions, respectively. After 14 days for tumor growth to a size of  $\sim 100 \text{ mm}^3$ , the magnetoplex containing 40  $\mu\text{g}$  Cy5-labeled DNA was intravenously injected via the tail vein. After injection, a static magnet was placed at the mice's right hind leg region for 20 min. Optical images of the tumor-bearing mice were taken using an IVIS Spectrum System 3D (Caliper Life Sciences, Hopkinton, MA). The tumor-bearing nude mice were anesthetized with 2.5% isoflurane using XGI-8 Gas Anesthesia System (Caliper Life Sciences) before being placed into the imaging chamber and imaged at various time points after the tail-vein injection of the magnetoplex containing Cy5-labeled DNA. Relevant organs, tissues, and tumors were dissected from the mice and imaged immediately to determine biodistribution at a time point of 48 h.

### Statistical analysis

Means and standard deviations (SD) of the data were calculated. Differences between the groups were tested using Student's *t*-test, and  $P < 0.05$  was considered to be significant.

## RESULTS AND DISCUSSION

### Preparation and characterization of CPIO

The synthesis of CP and PAAIO is referred to in our previous reports.<sup>33, 44, 45</sup> Briefly, CP was prepared by grafting PEI onto methylacetylated-CS with 70% methacrylation via a Michael addition method<sup>33</sup> and PAAIO was synthesized through a one-pot reaction between poly(acrylic acid) (PAA) and  $\text{Fe}_3\text{O}_4$ .<sup>44, 45</sup> CP with a high content of PEI (CP(H)) exhibited high transgene efficiency but showed high cytotoxicity.<sup>33</sup> To reduce the used amount of CP(H) for gene delivery, CP(H) was coated onto PAAIO (CPIO) through electrostatic interactions (Scheme 1). The positively-charged CPIO formed a magnetoplex with the negatively-charged DNA, which could reduce cytotoxicity and further enhance gene expression with an assisted magnetic field.

To obtain a stable CPIO, various weight ratios of CP and PAAIO were tested at 1:1, 2:1, and 4:1 in DD water of pH 6.8. No turbidity was observed when mixing solutions at these weight ratios. PAAIO had an average hydrodynamic diameter of ~60 nm and a negative zeta potential of

-15 mV. However, all CPIO at different weight ratios of CP and PAAIO had positive zeta potentials (Table S1). The positive zeta potential of CPIO implies the successful coating of CP onto the surface of PAAIO. The hydrodynamic diameters of CPIO decreased with an increase in CP feeding amount. They were ~162, 136, and 113 nm respectively for CP:PAAIO at the weight ratios of 1:1, 2:1, and 4:1 (Table S1). The CPIO with smaller particle sizes at the weight ratios of 2:1 and 4:1 were selected for transgene testing. The result demonstrates the CPIO at the weight ratio of 2:1 exhibited higher green fluorescence intensity than did 4:1 (Fig. S1). Thus, the CPIO prepared at this weight ratio (2:1) was adopted for later studies.

### **Characterization of CPIO/DNA magnetoplexes**

At w/w= 3, CPIO/DNA showed the largest hydrodynamic diameters (~400 nm) and nearly electrical neutrality, leading to particle aggregation. The hydrodynamic diameters were  $146 \pm 18$ ,  $93 \pm 7$ , and  $92 \pm 14$  nm for CPIO/DNA at the w/w ratios of 5, 10, and 15, respectively (Figure 1a). The particle size of CPIO/DNA at the w/w ratio of 5 dramatically decreased and showed a positive zeta potential of ~10 mV. After that, the zeta potential slightly increased with an increasing weight ratio of CPIO/DNA (Figure 1b). The morphological image of CPIO showed a cloud-like particle and CPIO/DNA a cluster formation (the insert of Figure 1a). The DNA binding ability of CPIO/DNA at a w/w ratio of 0.5 - 10 was tested using an agarose gel

electrophoresis retardation assay (Figure 1c). The result illustrates DNA was well complexed by CPIO at a w/w ratio of  $>1$ . To verify the protection of DNA against DNase I digestion, the electrophoretic mobility analysis of CPIO/DNA was tested after it had been left standing in 1U DNase I at RT for 1 h. A competition reagent of heparin was used to release DNA from CPIO/DNA. As shown in Figure 1(d), most of the DNA remained intact at a w/w ratio of  $\geq 3$  and degraded at the w/w ratio of 1 after 1 h of incubation with DNase I. Thus, we ensured the DNA was well protected by CPIO if a magnetoplex was prepared at a weight ratio of  $\geq 3$ .

### **Effect of a magnetic field on cellular uptake**

Magnet-assisted transfection has attracted considerable attention because it can rapidly assemble magnetoplexes to the surface of cells in the presence of a magnetic field and enhance gene expression. To understand the power of the assisted magnetic field on cellular uptake, pGL3-control was conjugated with a fluorescent Cy5 dye. The CPIO/Cy5-DNA at the w/w ratio of 5 was chosen to find an optimized condition for best cellular uptake into U87 cells using flow cytometry. A magnetic array was applied underneath a cell culture plate for 10, 20, and 30 mins. The amount of the internalized magnetoplex was maximized with an assisted magnetic field for 20 min. (Fig. S2). ICP-OES was used to analyze the iron content inside the U87 cells with and without the assisted magnetic field for this time point as well. In Figure 2(a), the internalized iron

amount of the cells exposed to CPIO/DNA at different w/w ratios was significantly higher as the external magnetic field was present. A similar result was observed in the cellular uptake of CPIO/DNA at w/w=5 using flow cytometry (Figure 2b). To directly visualize the magnetoplex inside the cells, we conjugated another fluorescent dye FITC onto CPIO. The fluorescent magnetoplex containing Cy5-labeled DNA and FITC-conjugated CPIO were simultaneously traced using CLSM. The cell nuclei were stained with Hoechst 33342 in blue. In Figure 2(c), we clearly observed more fluorescent spots of FITC-CPIO and Cy5-DNA in the cytoplasm as the magnetic field was applied. Thus, we concluded CPIO/DNA indeed accumulated in the cytoplasm rapidly with an assisted magnet for 20 min. This optimized condition was adopted for later studies.

### **Cytotoxicity.**

CPIO showed negligible cytotoxicities in all test concentrations against 293T, CRL-5802, and U87 cells (Fig. S3). The cell viabilities of CPIO/DNA were also tested against these three cell lines. At a w/w ratio of 3 - 15 with the magnetic field for 20 min, the CPIO/DNA-treated cells showed lower cytotoxicity than did the PolyMag-treated cells (Figure 3). The cell viability of CPIO/DNA was  $\geq 90\%$  in the three cell lines but that of PolyMag/DNA was  $<70\%$  in 293T cells, and  $\sim 80\%$  in CRL-5802 and U87 cells. This implies CPIO was superior to PolyMag for

future developments in biomedicine because of the lower cytotoxicity.

### ***In vitro* gene transfection**

To evaluate the effect of the magnetic field on gene expression, 293T, CRL-5802, and U87 cells were exposed to CPIO/DNA at a w/w ratio of 3 - 15 with or without an external magnetic field. A commercial magnetofection reagent-PolyMag and the gold standard of the nonviral gene vectors-PEI-25K were used as positive controls. PEGFP-C1 was qualitatively used for efficient GFP expression using fluorescence microscopy (Fig. S4) and pGL3-control plasmid was quantitatively used for luciferase expression using a plate reader (Figure 4). The luciferase expression was investigated with or without 10% FBS in the three cell lines. Without applying the magnetic field, the transfection efficiency of CPIO/DNA in U87 cells consistently increased with increasing w/w ratios whether 10% FBS was present or not. With the assisted magnetic field, the transfection efficiency of CPIO/DNA was comparable with that of PolyMag/DNA in the absence of 10% FBS (Figure 4a) but significantly higher than those of PolyMag/DNA and PEI-25K/DNA in the presence of 10% FBS (Figure 4d). In CRL-5802 cells, the transfection efficiency was higher with than without the assisted magnetic field at a CPIO/DNA weight ratio of  $\leq 10$  in the absence of 10% FBS (Figure 4b). In the presence of 10% FBS, all gene carrier materials showed lower transgene expression, even when the assisted magnetic field was applied

(Figure 4e). However, in 293T cells, the decreased transfection efficiencies in the presence of 10% FBS were not as serious as those in U87 cells and CRL-5802 cells. CPIO/DNA showed a low magnetofection effect relative to PolyMag in the condition without FBS (Figure 4c). Nevertheless, with FBS, the transfection efficiency of CPIO/DNA was comparable at w/w= 10, 15 but higher at w/w= 3, 5 as compared with PolyMag/DNA or PEI/DNA. Although the trend of gene expression in different cell lines from the highest to the lowest was 293T cells, U87 cells, and CRL-5802 cells, the U87 cells showed the most improvement in transfection efficiency when an external magnetic field was applied in the presence of FBS. Thus, we tentatively concluded CPIO seems a more efficient megneto-gene carrier than PolyMag in the glioma cell line.

### **Magnetofection trafficking**

As previously mentioned, an external magnet helped magnetoplexes rapidly internalize into cells and enhanced gene expression remarkably. To investigate the time course of magnetofection efficiency, the green fluorescence expression of pEGFP was traced by CLSM and the luciferase activity of pGL3 was measured using a microplate scintillation and luminescence counter. The optimized weight ratio of CP/DNA at w/w= 7 and CPIO/DNA at w/w= 5 without the assisted magnetic field were acquired as reference groups and the CPIO/DNA with an assisted magnetic field for 20 mins was a test group. U87 cells were post-incubated and traced at different time

periods of 3 - 48 h. In Figure 5(a), U87 cells exposed to CPIO/DNA with an assisted magnetic field clearly showed green fluorescent spots after 3h of post-incubation but those exposed to CP/DNA and CPIO/DNA without the magnetic field did not. The green fluorescence intensity increased with time of post-incubation in all three systems, but CPIO/DNA exhibited significant GFP expression with an assisted magnetic field relative to the other two groups at every time point. The quantitative transfection efficiencies of the three systems were measured by luciferase-mediated luminescence as well (Figure 5b). As expected, the CPIO/DNA with the assisted magnetic field showed the highest level of luciferase expression among the test groups. As compared with PolyMag, the CPIO with the assisted magnetic field not only accelerated gene expression, but magnificently enhanced the transfection efficiency.

### **MiRNA expression**

MiR-128 is an important miRNA sequence enriched in normal brain tissue and down-regulated in gliomas.<sup>25</sup> It can inhibit tumor proliferation, migration, and invasion.<sup>47</sup> Thus, we constructed a plasmid encoding miR-128 precursor named pMIRNA-128 and tested its potency using CPIO as a delivery carrier. A lentivector-based microRNA precursor construct, pMIRNA-128, contains CMV promoter for transcription of cloned miR-128. Besides, downstream transcript containing copGFP fluorescent marker sequence driven by EF1  $\alpha$

promoter could be used as a reporter gene to directly illustrate transfection efficiency. Magnetofection-mediated miR-128 expression was visualized using fluorescence *in situ* hybridization (FISH). In Figure 6(a), the red fluorescence of Cy5-labeled probe was observed in the cytoplasm of U87 cells. This result indicates CPIO as well as PolyMag could successfully transfect pMIRNA-128 into U87 cells. However, it seems CPIO had a higher potency than PolyMag did because more red fluorescent spots were observed.

Another method was used to test miR-128 expression using a miRNA plate array which was coated with a biotinated oligo-miRNA detector. The extracted RNA from transfected cells was added to the plate and captured with an immobilized oligo-antisense sequence. The miRNA expression was detected using a streptavidin-HRP conjugate and a chemiluminescent substrate. In Figure 6(b), CPIO and PolyMag without the magnetic field had miRNA expression levels of ~1.5 fold relative to the control group. In the presence of the magnetic field, the miRNA expression level of CPIO/pDNA was ~1.5 fold higher than that without the assisted magnetic field and ~2.6 fold higher than the control group. In contrast, an increase in the miRNA expression level of PolyMag/pDNA was insignificant with an assisted magnetic field.

The oncogene Bmi-1 is a direct target of miR-128 and leads to a growth in glioma.<sup>25</sup> MiR-128 is highly associated with tumor suppression and strong affects Bmi-1 down-regulation.<sup>25, 48</sup> In addition, miR-128 was reported to inhibit Akt activation in human glioblastoma and

glioma-initiating neural glioblastoma cells.<sup>49</sup> Akt is a serine/threonine kinase and is highly associated with cell growth, cell differentiation, survival, and anti-apoptosis. The constitutive activation of Akt shows the chemo-resistance of tumor cells.<sup>50</sup> Therefore, we investigated the transfection effect of pMIRNA-128 on Akt expression. As shown in Figure 6(c), CPIO/pDNA with the magnetic field suppressed Akt and p-Akt expression more notably than PolyMag/pDNA with the magnetic field and CPIO/pDNA without the magnetic field.

### **Biodistribution**

To evaluate the *in vivo* magneto-induced uptake of a magnetoplex, the biodistribution of CPIO/Cy5-DNA was studied in nude mice with U87-xenografted tumors on the right and left hind leg regions. A static magnet was placed on the right tumor of the mice (Figure 7a). We optically imaged the Cy5 dye intensity in the U87 xenograft-bearing mice at different time points after we had injected the magnetoplex containing Cy5-DNA via the tail-vein. The fluorescence intensity of Cy5-DNA at both the tumor sites increased with increasing circulation time after 3h (Figure 7b). Nevertheless, the one with the assisted magnet showed the higher fluorescence intensity. The relevant organs, tissues, and tumors were dissected from the mice at 48 h after instillation and optically imaged immediately to determine the remaining fluorescence intensity. In Figure 7c, we clearly observed Cy5-DNA fluorescence at the tumor site exposed to the

magnetic field. In addition to the enhanced permeation and retention effect (EPR) at the tumor site, CPIO/pDNA could trigger the CD44-mediated endocytosis and enhanced the cellular uptake into U87 cells because the CP moiety in CPIO indeed promote CD44-mediated endocytosis for enhanced gene delivery.<sup>33</sup> This *in vivo* result was consistent with that found in the cellular uptake studies using a flow cytometer and a CLSM.

## CONCLUSIONS

CPIO was successfully prepared by combining CP and PAAIO. With an assisted magnetic field, effective magnetofection of CPIO/DNA was obtained in 293T, CRL-5802, and U87 cells. Through magnetofection, CPIO enhanced transfection efficiency and accelerated gene expression. In addition, CPIO showed the least cytotoxicity against the three cell lines. In pMIRNA-128 delivery, CPIO/DNA indeed expressed miR-128 higher than PolyMag/DNA. From *in vivo* study, CPIO/Cy5-DNA localized DNA at the tumor site where the magnetic field was applied for 20 mins. Herein, we developed a non-cytotoxic and highly efficient CPIO as a magnetofection carrier for potential glioma therapy.

## ACKNOWLEDGEMENTS

We are grateful for the financial support from the Ministry of Science and Technology of Taiwan

(MOST103-2325-B-037-001 and MOST103-2320-B-037-012-MY3). This study is also supported by “Aim for the Top 500 Universities Grant (KMU-DT103007)” and by “NSYSU-KMU Joint Research Project, (NSYSUKMU 104-P026)” from Kaohsiung Medical University. We appreciate the experiment support of confocal laser scanning microscope from Center for Research Resources and Development of KMU.

## REFERENCES

1. A. Kwiatkowska, M. S. Nandhu, P. Behera, E. A. Chiocca and M. S. Viapiano, *Cancers (Basel)*, 2013, 5, 1271-1305.
2. S. Koo, G. S. Martin, K. J. Schulz, M. Ronck and L. G. Toussaint, *BMC Cancer*, 2012, 12, 143.
3. H. Xin, X. Jiang, J. Gu, X. Sha, L. Chen, K. Law, Y. Chen, X. Wang, Y. Jiang and X. Fang, *Biomaterials*, 2011, 32, 4293-4305.
4. W. M. Pardridge, *Drug Discov. Today*, 2001, 6, 381-383.
5. W. M. Pardridge, *Jpn. J. Pharmacol.*, 2001, 87, 97-103.
6. W. M. Pardridge, *Drug Discov. Today*, 2001, 6, 1-2.
7. C. K. Chen, W. C. Law, R. Aalinkeel, B. Nair, A. Kopwitthaya, S. D. Mahajan, J. L. Reynolds, J. Zou, S. A. Schwartz, P. N. Prasad and C. Cheng, *Adv. Healthc. Mater.*, 2012, 1, 751-761.
8. H. Yin, R. L. Kanasty, A. A. Eltoukhy, A. J. Vegas, J. R. Dorkin and D. G. Anderson, *Nat. Rev. Genet.*, 2014, 15, 541-555.
9. S. H. Hu, T. Y. Hsieh, C. S. Chiang, P. J. Chen, Y. Y. Chen, T. L. Chiu and S. Y. Chen, *Adv. Healthc. Mater.*, 2014, 3, 273-282.
10. D. W. Pack, A. S. Hoffman, S. Pun and P. S. Stayton, *Nat. Rev. Drug Discov.*, 2005, 4, 581-593.
11. M. A. Mintzer and E. E. Simanek, *Chem. Rev.*, 2009, 109, 259-302.
12. Y. Yang, F. Liu, X. Liu and B. Xing, *Nanoscale*, 2013, 5, 231-238.
13. J. J. Rychak and A. L. Klibanov, *Adv. Drug Deliv. Rev.*, 2014, 72, 82-93.
14. I. Lentacker, B. G. De Geest, R. E. Vandenbroucke, L. Peeters, J. Demeester, S. C. De

- Smedt and N. N. Sanders, *Langmuir*, 2006, 22, 7273-7278.
15. F. Scherer, M. Anton, U. Schillinger, J. Henke, C. Bergemann, A. Kruger, B. Gansbacher and C. Plank, *Gene Ther.*, 2002, 9, 102-109.
  16. S. Prijic and G. Sersa, *Radiol. Oncol.*, 2011, 45, 1-16.
  17. S. J. Huang, J. H. Ke, G. J. Chen and L. F. Wang, *J. Mate. Chem. B*, 2013, 1, 5916-5924.
  18. C. A. Smith, J. de la Fuente, B. Pelaz, E. P. Furlani, M. Mullin and C. C. Berry, *Biomaterials*, 2010, 31, 4392-4400.
  19. S. Huth, J. Lausier, S. W. Gersting, C. Rudolph, C. Plank, U. Welsch and J. Rosenecker, *J. Gene Med.*, 2004, 6, 923-936.
  20. W. M. Liu, Y. N. Xue, W. T. He, R. X. Zhuo and S. W. Huang, *J. Controlled Release*, 2011, 152 Suppl 1, e159-160.
  21. S. L. Sun, Y. L. Lo, H. Y. Chen and L. F. Wang, *Langmuir*, 2012, 28, 3542-3552.
  22. D. M. Pereira, P. M. Rodrigues, P. M. Borralho and C. M. Rodrigues, *Drug Discov. Today*, 2013, 18, 282-289.
  23. A. E. Pasquinelli, *Nat. Rev. Genet.*, 2012, 13, 271-282.
  24. S. A. Ciafre, S. Galardi, A. Mangiola, M. Ferracin, C. G. Liu, G. Sabatino, M. Negrini, G. Maira, C. M. Croce and M. G. Farace, *Biochem. Biophys. Res. Commun.*, 2005, 334, 1351-1358.
  25. J. Godlewski, M. O. Nowicki, A. Bronisz, S. Williams, A. Otsuki, G. Nuovo, A. RayChaudhury, H. B. Newton, E. A. Chiocca and S. Lawler, *Cancer Res.*, 2008, 68, 9125-9130.
  26. Z. M. Shi, J. Wang, Z. P. Yan, Y. P. You, C. Y. Li, X. Qian, Y. Yin, P. Zhao, Y. Y. Wang, X. F. Wang, M. N. Li, L. Z. Liu, N. Liu and B. H. Jiang, *PLoS One*, 2012, 7.
  27. S. Wuchty, D. Arjona, A. G. Li, Y. Kotliarov, J. Walling, S. Ahn, A. Zhang, D. Maric, R. Anolik, J. C. Zenklusen and H. A. Fine, *PLoS One*, 2011, 6.
  28. Y. Bo, G. Guo and W. Yao, *J. Neurooncol.*, 2013, 112, 27-37.
  29. R. Paulmurugan, *Theranostics*, 2013, 3, 927-929.
  30. Y. K. Adlakha and N. Saini, in *Cell. Mol. Life Sci.*, 2010/10/07 edn., 2011, vol. 68, pp. 1415-1428.
  31. Y. Zhang, T. Chao, R. Li, W. Liu, Y. Chen, X. Yan, Y. Gong, B. Yin, B. Qiang, J. Zhao, J. Yuan and X. Peng, *J. Mol. Med. (Berl)*, 2009, 87, 43-51.
  32. W. Hwang, S. Son, J. Jang, H. Youn, S. Lee, D. Lee, Y. S. Lee, J. M. Jeong, W. J. Kim and D. S. Lee, *Biomaterials*, 2011, 32, 4968-4975.
  33. Y. L. Lo, K. H. Sung, C. C. Chiu and L. F. Wang, *Mol. Pharm.*, 2013, 10, 664-676.
  34. T. Kurosaki, T. Kitahara, S. Kawakami, K. Nishida, J. Nakamura, M. Teshima, H. Nakagawa, Y. Kodama, H. To and H. Sasaki, *Biomaterials*, 2009, 30, 4427-4434.

35. A. Pathak, P. Kumar, K. Chuttani, S. Jain, A. K. Mishra, S. P. Vyas and K. C. Gupta, *ACS Nano*, 2009, 3, 1493-1505.
36. A. Bertolotto, G. Rocca and D. Schiffer, *J. Neurol. Sci.*, 1990, 100, 113-123.
37. M. C. Kuppner, E. Van Meir, T. Gauthier, M. F. Hamou and N. Detribolet, *Int. J. Cancer*, 1992, 50, 572-577.
38. S. Nagasaka, K. K. Tanabe, J. M. Bruner, H. Saya, R. E. Sawaya and R. S. Morrison, *J. Neurosurg.*, 1995, 82, 858-863.
39. S. M. Ranunolo, V. Ladeda, S. Specterman, M. Varela, J. Lastiri, A. Morandi, E. Matos, E. Bal de Kier Joffe, L. Puricelli and M. G. Pallotta, *J. Surg. Oncol.*, 2002, 79, 30-35; discussion 35-36.
40. A. Jong, C. H. Wu, I. Gonzales-Gomez, K. J. Kwon-Chung, Y. C. Chang, H. K. Tseng, W. L. Cho and S. H. Huang, *J. Biol. Chem.*, 2012, 287, 15298-15306.
41. A. Jong, C. H. Wu, G. M. Shackelford, K. J. Kwon-Chung, Y. C. Chang, H. M. Chen, Y. Ouyang and S. H. Huang, *Cell. Microbiol.*, 2008, 10, 1313-1326.
42. A. Merzak, S. Koocheckpour and G. J. Pilkington, *Cancer Res.*, 1994, 54, 3988-3992.
43. L. F. Wang, S. S. Shen and S. C. Lu, *Carbohydr. Polymers*, 2003, 52, 389-396.
44. J. H. Ke, J. J. Lin, J. R. Carey, J. S. Chen, C. Y. Chen and L. F. Wang, *Biomaterials*, 2010, 31, 1707-1715.
45. J. J. Lin, J. S. Chen, S. J. Huang, J. H. Ko, Y. M. Wang, T. L. Chen and L. F. Wang, *Biomaterials*, 2009, 30, 5114-5124.
46. Y. L. Lou, Y. S. Peng, B. H. Chen, L. F. Wang and K. W. Leong, *J. Biomed. Mater. Res. A*, 2009, 88, 1058-1068.
47. L. Lin, X. Chen, X. Peng, J. Zhou, H. F. Kung, M. C. Lin and S. Jiang, *Oncol. Rep.*, 2013, 30, 1239-1248.
48. P. Dong, Y. Konno, H. Watari, M. Hosaka, M. Noguchi and N. Sakuragi, *J. Transl. Med.*, 2014, 12, 231.
49. T. Papagiannakopoulos, D. Friedmann-Morvinski, P. Neveu, J. C. Dugas, R. M. Gill, E. Huillard, C. Liu, H. Zong, D. H. Rowitch, B. A. Barres, I. M. Verma and K. S. Kosik, *Oncogene*, 2012, 31, 1884-1895.
50. I. L. Lin, H. L. Chou, J. C. Lee, F. W. Chen, Y. Fong, W. C. Chang, H. W. Huang, C. Y. Wu, W. T. Chang, H. M. Wang and C. C. Chiu, *Cancer Cell Int.*, 2014, 14, 1.

### Figure Captions

**Scheme 1.** A schematic illustration of chondroitin sulfate-polyethylenimine (CP)-coated superparamagnetic iron oxide nanoparticles (CPIO) mediated magnetofection.

**Figure 1. Characterization of CPIO/DNA magnetoplexes.** DLS analysis of (a) hydrodynamic diameters and (b) zeta potentials of CPIO/DNA; (c) Agarose gel electrophoresis analysis of DNA retention and (d) DNase I digestion assay of CPIO/DNA magnetoplexes prepared at various w/w ratios. The CPIO/DNA magnetoplexes were incubated with 1U DNase I followed by treated with 25% heparin to release DNA from the magnetoplexes.

**Figure 2. Effect of a magnetic field on the cellular uptake of CPIO/DNA into U87 cells.** (a) Internalized iron content quantified by ICP-OES ( $n=3$ ,  $*p < 0.05$ ); (b) Flow cytometric diagrams and (c) CLSM images. U87 cells were exposed to CPIO/DNA at various w/w ratios with (w) or without (w/o) the magnetic field for 20 mins. Green: FITC-conjugated CPIO; Red: Cy5-labeled DNA; Blue: Hoechst 33342-stained cell nuclei.

**Figure 3. MTT assay of cytotoxicity.** CPIO/DNA were prepared at various w/w ratios with (w) or without (w/o) the magnetic field for 20 mins followed by 48 h post-incubation against (a) U87, (b) CRL-5802, and (c) 293T cells. PEI-25K/DNA was prepared at an N/P ratio of 10 and PolyMag/DNA was prepared according to the manufacturer's protocol with an assisted magnetic field for 20 mins.

**Figure 4. Transfection efficiency measured by luciferase expression.** CPIO/DNA were prepared at various w/w ratios with (w) or without (w/o) the magnetic field for 20 mins against (a, d) U87, (b, e) CRL-5802, and (c, f) 293T cells in the absence (a-c) or presence (d-f) of 10% FBS. PEI-25K/DNA was prepared at an N/P ratio of 10 and

PolyMag/DNA was prepared according to manufacturer's protocol with the assisted magnetic field for 20 mins.

**Figure 5. Transfection efficiency in U87 cells.** (a) The CLSM image of green fluorescence expression of pEGFP. Cell nuclei were stained with Hoechst. (b) Luciferase activities of CPIO/DNA at w/w=5 with (w) or without (w/o) an assisted magnetic field for 20 mins followed by post-incubation for different time periods of 3 - 48 h. CP/DNA was tested at N/P=7 and PolyMag/DNA was prepared according to the manufacturer's protocol with the assisted magnetic field for 20 mins.

**Figure 6. MiRNA-128 expression in U87 cells.** The transgene expression of miRNA-128 was measured by (a) fluorescence in situ hybridization (FISH) with an assisted magnetic field and (b) a miRNA assay plate kit. CPIO/DNA was prepared at w/w=5 with (w) or without (w/o) an assisted magnetic field for 20 mins (n=3, \* $p < 0.05$ ). (c) The western blot analysis of pAKT, AKT, and Bax protein expression. GAPDH was used as an internal control. PolyMag/DNA was prepared according to the manufacturer's protocol with the assisted magnetic field for 20 mins.

**Figure 7.** (a) U87-xenografted on the right and left hind leg regions of a male Balb/c mouse. A static magnet was placed on the right tumor of the mouse. (b) CPIO/Cy5-DNA distribution in the mouse (6 weeks old) using a near-infrared noninvasive optical imaging system. (c) Fluorescence intensity of isolated tissues from the mouse at 48 h.

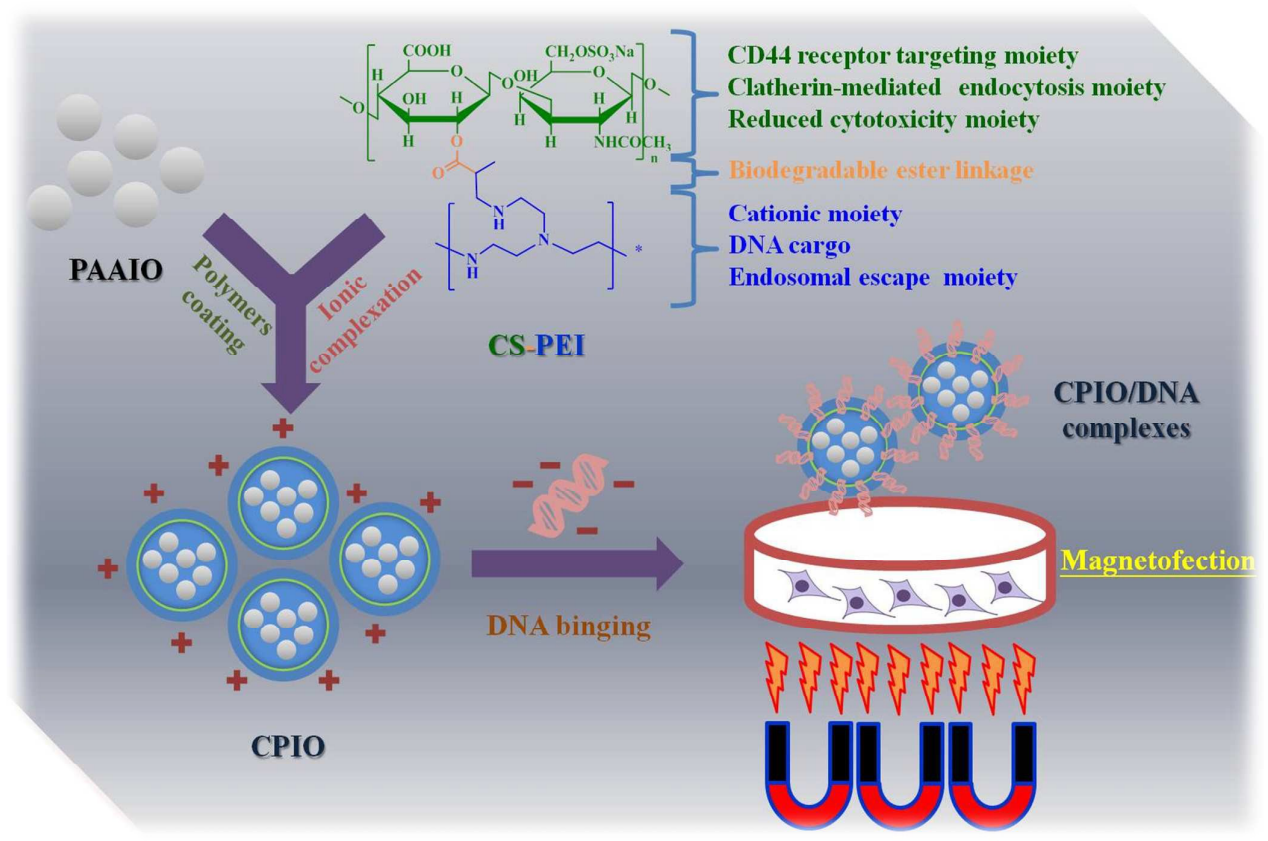


Fig. 1.

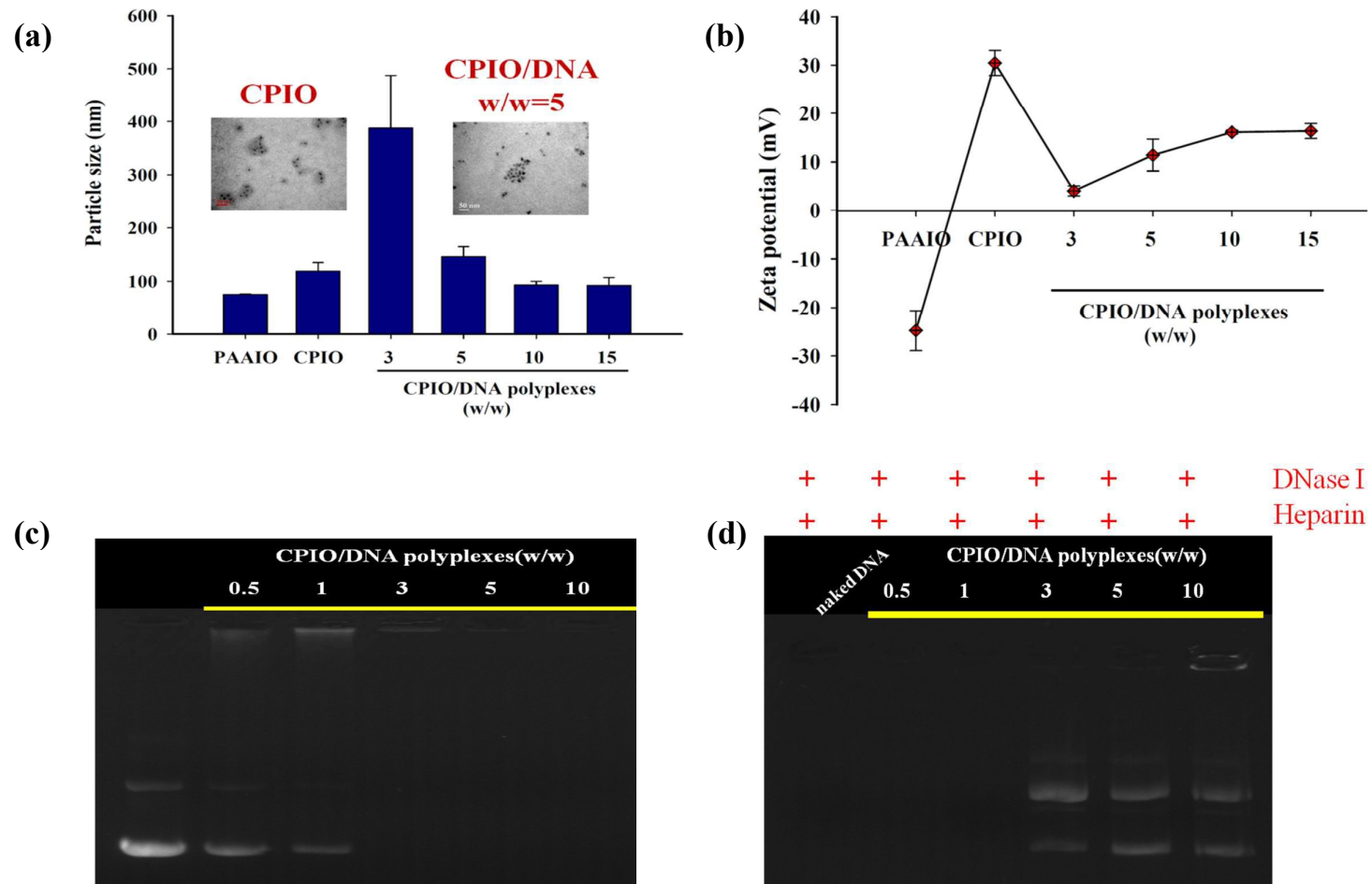


Fig. 2.

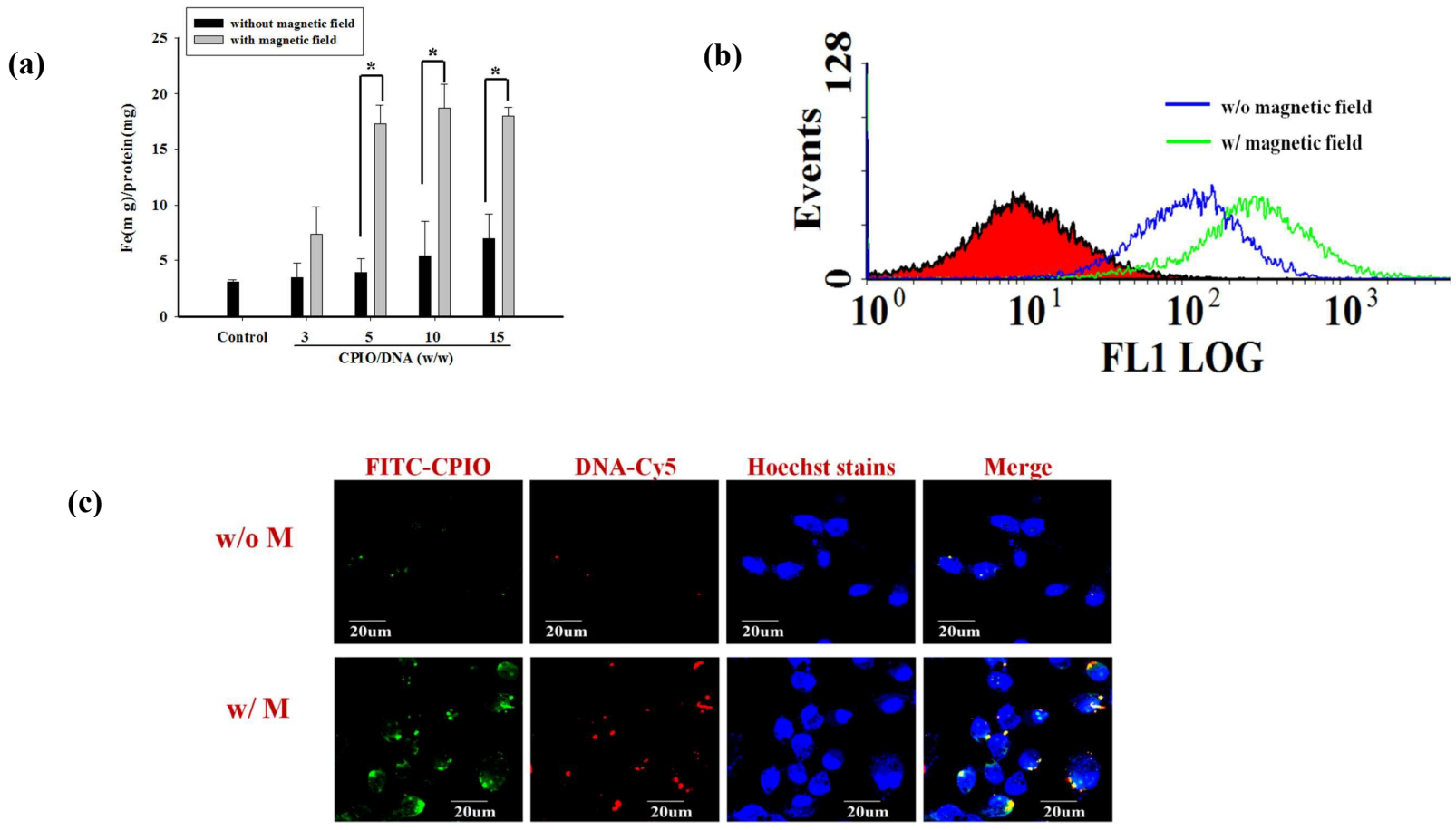


Fig. 3.

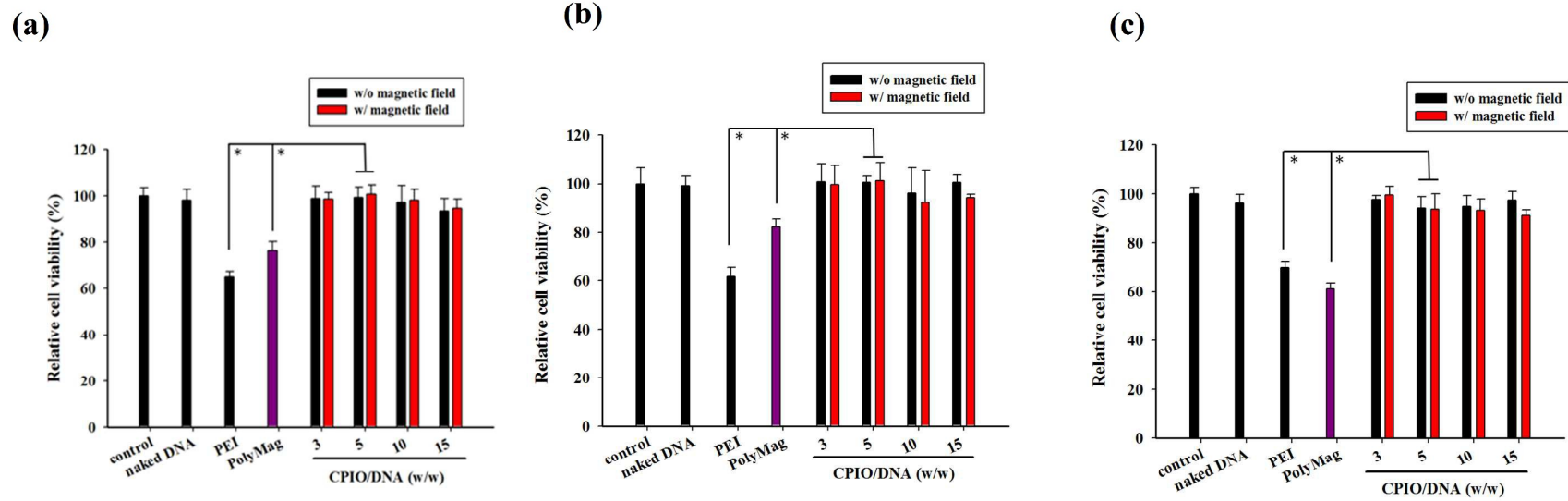


Fig. 4.

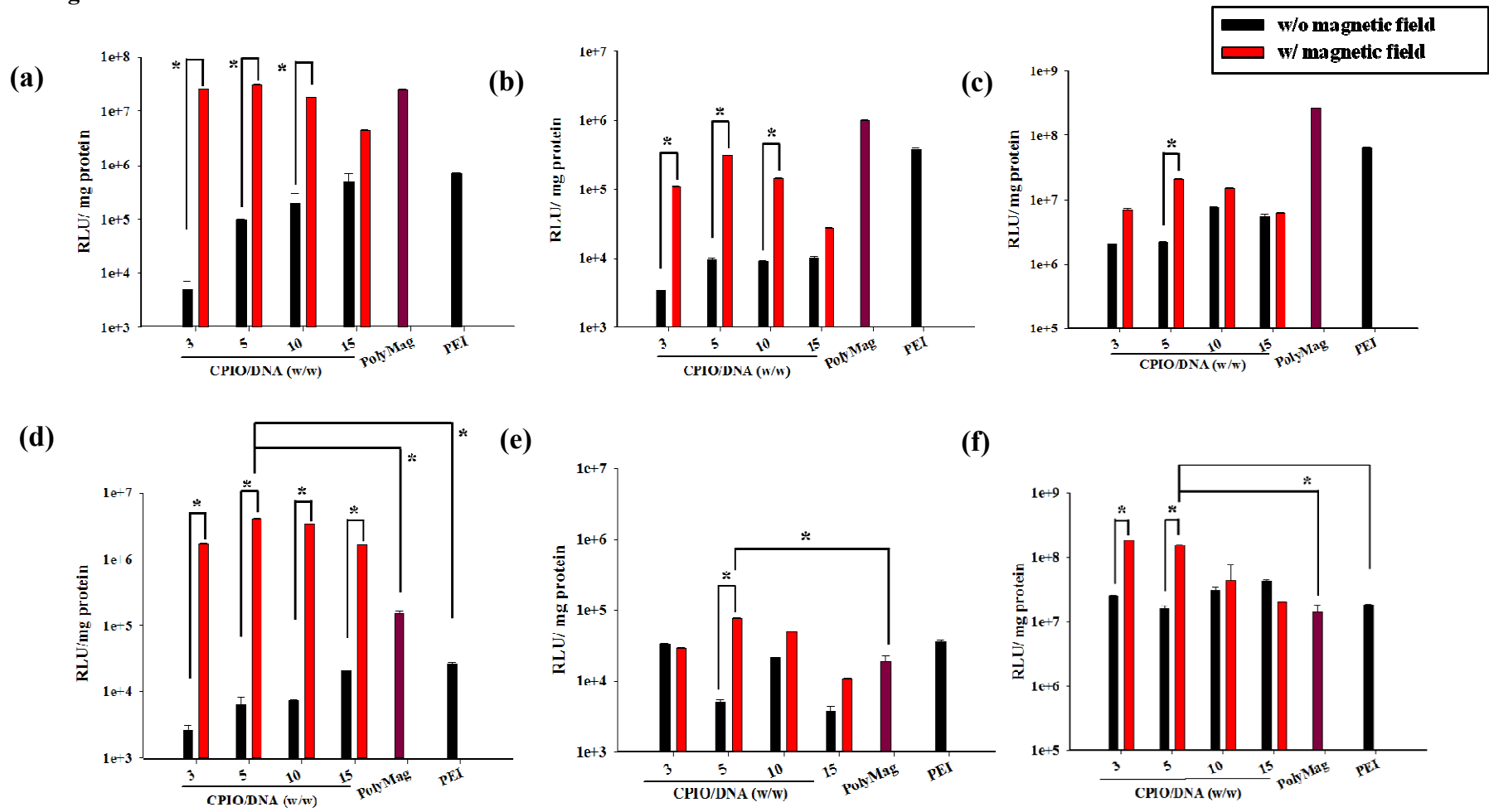


Fig. 5.

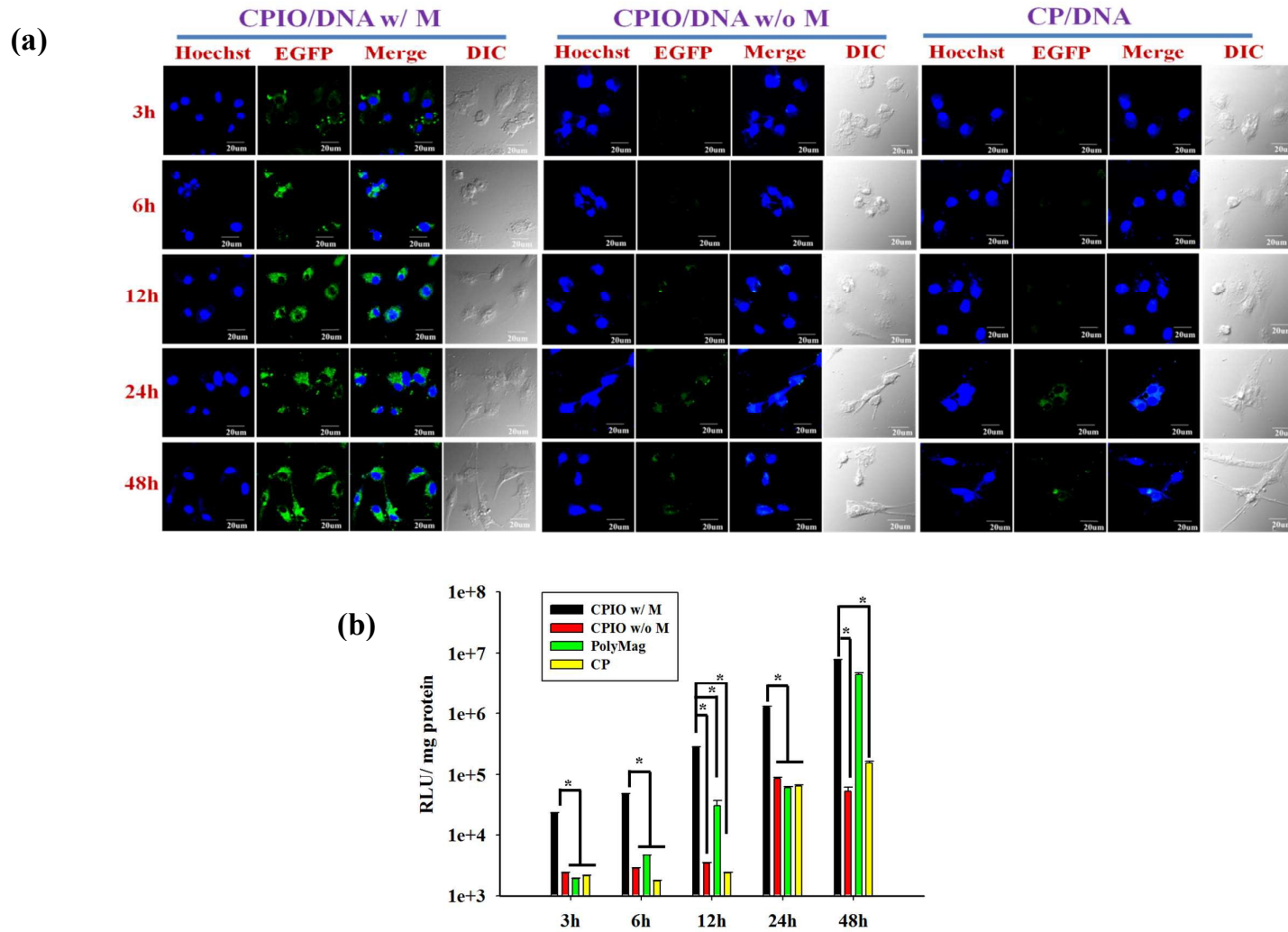


Fig. 6.

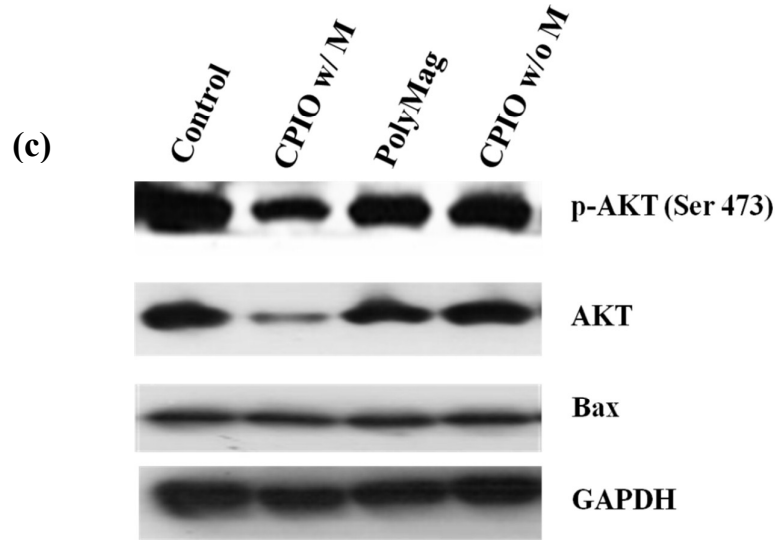
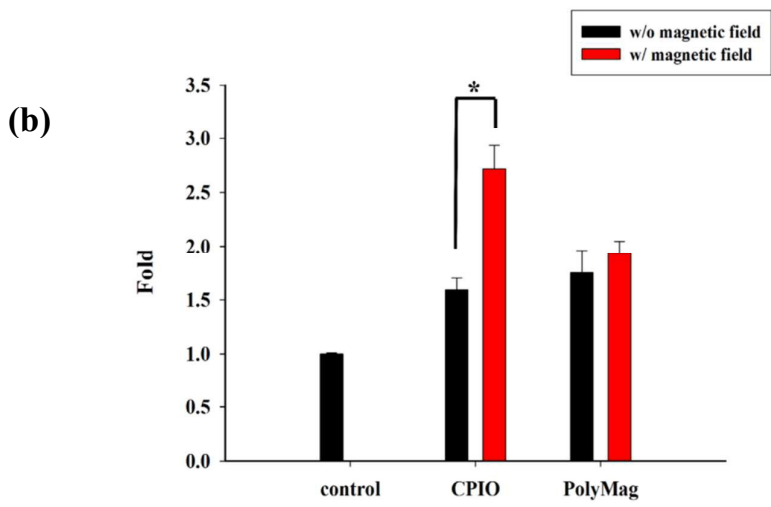
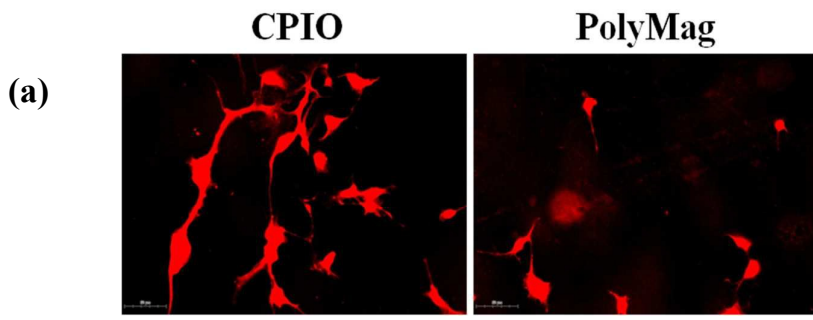


Fig. 7

